Research Article | Vol. 29, No. 3 / 1 February 2021 / Optics Express 3928
Optics EXPRESS

Generation of quantum entanglement based on electromagnetically induced transparency media

YOU-LIN CHUANG,[1] RAY-KUANG LEE,[1,2,3,*] AND ITE A. YU[3]

[1]Physics Division, National Center for Theoretical Sciences, Hsinchu 30013, Taiwan
[2]Institute of Photonics Technologies, National Tsing Hua University, Hsinchu 300, Taiwan
[3]Department of Physics, National Tsing Hua University, Hsinchu 30013, Taiwan
[*]rklee@ee.nthu.edu.tw

Abstract: Quantum entanglement is an essential ingredient for the absolute security of quantum communication. Generation of continuous-variable entanglement or two-mode squeezing between light fields based on the effect of electromagnetically induced transparency (EIT) has been systematically investigated in this work. Here, we propose a new scheme to enhance the degree of entanglement between probe and coupling fields of coherent-state light by introducing a two-photon detuning in the EIT system. This proposed scheme is more efficient than the conventional one, utilizing the ground-state relaxation (population decay or dephasing) rate to produce entanglement or two-mode squeezing which adds far more excess fluctuation or noise to the system. In addition, maximum degree of entanglement at a given optical depth can be achieved with a wide range of the coupling Rabi frequency and the two-photon detuning, showing our scheme is robust and flexible. It is also interesting to note that while EIT is the effect in the perturbation limit, i.e. the probe field being much weaker than the coupling field and treated as a perturbation, there exists an optimum ratio of the probe to coupling intensities to achieve the maximum entanglement. Our proposed scheme can advance the continuous-variable-based quantum technology and may lead to applications in quantum communication utilizing squeezed light.

1. Introduction

Continuous-variable (CV) quantum entanglement is an important resource which has been paid great attention in modern quantum optics and quantum information sciences, possessing many potential applications in quantum teleportation [1], quantum key distribution [2], quantum communication [3,4], quantum information processing [5], etc. Carrying quantum information onto the quadratures of optical fields, such as amplitude and phase, has higher tolerance to dissipation during light propagation processes. In addition, CV quantum entanglement can be realized in other degree of freedom of optical fields, for instance, the polarization state of light has also been extensively studied in CV regime by transforming the quadrature entanglement onto polarization basis [6–9], and the quadrature entanglement using quantum orbital angular momentum with spatial Laguerre-Gauss mode has been discussed in experiment [10]. Furthermore, CV entanglement light source is essential in quantum imaging [11–13], which is an extension of quantum nature to transverse spatial degree of freedom. According to these previous researches, it is believed that optical field in CV entanglement plays an ideal information carrier, which is robust in quantum information sciences.

In order to generate entangled light, it is well known that using of optical nonlinear crystal is a typical scheme to generate light sources in CV regime. In theory, quantum correlation based on nondegenerate parametric oscillation was proposed [14]. Later, the generation of CV entanglement with nondegenerate parametric amplification was first observed in experiment

#413217 https://doi.org/10.1364/OE.413217
Journal © 2021 Received 26 Oct 2020; revised 13 Jan 2021; accepted 19 Jan 2021; published 25 Jan 2021

Optics EXPRESS

by Ou *et al.* in 1992 [15]. Recently, the CV quantum entanglement at a telecommunication wavelength of 1550 nm had been realized using nondegenerate optical parametric amplifer [16]. On the other hand, mixing two independent squeezed lights which are generated from optical parametric amplifiers individually provides a practical method to generate quadrature entanglement [17]. These studies above clearly indicate that there is a connection between nonlinear optical processes and CV entanglement generation, so that the integration of all optical elements on chip has been proposed in order to further approach the goal of implementation of quantum computer in future [18].

Although the generation of quantum light sources from optical parametric processes, especially using $\chi^{(2)}$ optical susceptibility of nonlinear crystal is popular, the light-matter interaction strength is difficult to control. In contrast, the nonlinear optical processes based on the interactions between fields and atomic systems can produce not only large amounts of quantum correlations between intense fields, but also controllability with accessible physical parameters. Recent decades, research reported on entangled light generation by four-wave mixing (FWM) has been intensely studied in hot atomic vapors [19–25]. Moreover, it has some potential applications, including the production of multiple quantum correlated beams [26], enhancement of the degree of entanglement [27], quantum metrology [28], etc. Meanwhile, electromagnetically induced transparency (EIT) [29] which is a coherent medium also plays an important role in atom-field interactions. Some peculiar features such as low-absorption, slow-light [30] and quantum memory [31–33] make EIT to be a promising ingredient in the development of quantum technologies. In the scenario, quantum optical pulse propagation in EIT [34], quantum squeezing generation in coherent population trapping media [35], large cross-phase modulation at few-photon level [36], and quantum correlated light generation as well as multiple fields correlation have been actively studied [37–46].

CV quantum entanglement arising from atom-field interactions is a good platform to investigate the connections between quantum coherence and correlations. Despite the fact that many papers have discussed the quantum entanglement generation in EIT systems, a systematic understanding of the physics behind the entanglement generation is still lacking. In this paper, we will discuss about the following questions: how do the tunable physical parameters in EIT system, which are photon-detunings, field Rabi frequencies, and atomic optical density, influence the entanglement degree between interacting fields? And how is the entanglement affected by the "EIT degree", which is related to ratio between two interacting field strengths. By solving the coupled equations of atomic and field operators numerically, we are able to study these questions.

The paper has been organized in the following way. In Sec. II, we start from a standard analysis of typical EIT interaction Hamiltonian, and derive the equations of motion for atomic operators, as well as the propagation equations for two quantized fields. The results from numerical calculation are given in Sec. III. Then, to reveal the underline physics, Sec. IV is concerned with the analytical approach for the output entanglement. Finally, a conclusion is given in Sec. V.

2. Theoretical model

We consider a collection of atoms having the three-level Λ-type configuration as shown in Fig. 1(a). Two ground states $|1\rangle$ and $|2\rangle$ are coupled to the common excited state $|3\rangle$ by probe and coupling fields, respectively. The Rabi frequency of probe field Ω_p is much weaker than that of the coupling Ω_c, and the whole system forms a standard EIT. The one-photon detuning of probe and coupling fields are defined by $\Delta_p = \omega_p - \omega_{31}$ and $\Delta_c = \omega_c - \omega_{32}$, where ω_p and ω_c denote the light frequencies of probe and coupling, and $\omega_{\mu\nu} \equiv (E_\mu - E_\nu)/\hbar$ is the energy difference between any two states $|\mu\rangle$ and $|\nu\rangle$. The two-photon detuning is an important parameter in EIT system, defined by $\delta = \Delta_p - \Delta_c$. The decay rates from $|3\rangle$ to the two ground states are Γ_1 and Γ_2, which are assumed to be the same in this work, so that we have $\Gamma_1 = \Gamma_2 = \Gamma/2$, where Γ is the total decay rate of $|3\rangle$. The damping rate from $|2\rangle$ to $|1\rangle$ is Γ_{12}. In addition, due to some

Optics EXPRESS

practical effects such as atom collisions, we have to introduce the dephasing rate between two ground states, which is given by γ_p.

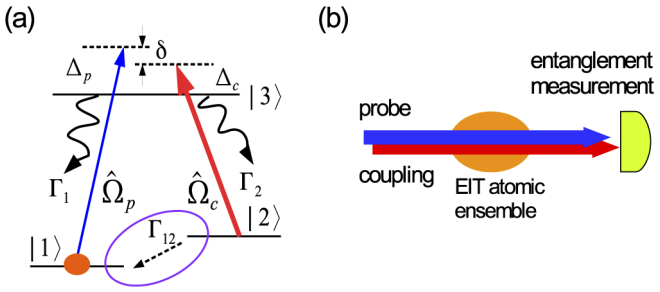

Fig. 1. (a) Atomic system configuration. (b) Probe and coupling are interacting with EIT atomic ensemble, and the entanglement measurement is performed at output.

The system is arranged as shown in Fig. 1(b). Probe and coupling fields are propagating along the same direction, illuminating the EIT atomic ensemble, which is cooled to several hundred micro-Kelvin. Both probe and coupling fields are coherent states at input, and the entanglement measurement is performed at output for the two fields after propagating though EIT ensemble. In experiments, a closed three-level system in the Λ-type configuration is feasible. For example, in the energy levels of rubidium-87 atoms, the two hyperfine ground states of $5S_{1/2}, F = 1$, $5S_{1/2}, F = 2$, and the excited state of $5P_{3/2}, F = 2$ can form the closed three-level system.

Next, we start to study the system theoretically. We write the atom-field interaction Hamiltonian $\hat{H}$ in the rotating wave approximation [34,35]

$$\begin{aligned}\hat{H} = &-\hbar\left(\Delta_p\hat{\sigma}_{33}(z,t) + \delta\hat{\sigma}_{22}(z,t)\right)\\ &-\hbar\left[\frac{\hat{\Omega}_p(z,t)}{2}\hat{\sigma}_{31}(z,t) + \frac{\hat{\Omega}_c(z,t)}{2}\hat{\sigma}_{32}(z,t) + H.c\right],\end{aligned} \tag{1}$$

in which $\hat{\Omega}_p(z,t) = g_p\hat{\mathcal{E}}_p(z,t)$ and $\hat{\Omega}_c(z,t) = g_c\hat{\mathcal{E}}_c(z,t)$, with $g_p = \mu_{13}\sqrt{\omega_p/2\epsilon_0 V\hbar}$ and $g_c = \mu_{23}\sqrt{\omega_c/2\epsilon_0 V\hbar}$, are the single photon Rabi frequencies of probe and coupling fields, respectively, corresponding to two dipole transitions μ_{13} and μ_{23}. Without loss of generality, we have assumed that $g_p = g_c \equiv g$, and $\hat{\mathcal{E}}_p$ and $\hat{\mathcal{E}}_c$ are dimensionless field operators, which satisfy bosonic commutation relations given by $\left[\hat{\mathcal{E}}_\mu, \hat{\mathcal{E}}_\mu^\dagger\right] = 1, \mu \in p, c$. According to the Hamiltonian in Eq. (2), we can write down the Heisenberg-Langevin equations for atomic operators.

$$\frac{\partial}{\partial t}\hat{\sigma}_{31} = -\left(\frac{\Gamma}{2} + i\Delta_p\right)\hat{\sigma}_{31} - \frac{i}{2}(\hat{\sigma}_{11} - \hat{\sigma}_{33})\hat{\Omega}_p^\dagger - \frac{i}{2}\hat{\Omega}_c^\dagger\hat{\sigma}_{21} + \hat{F}_{31}, \tag{2}$$

$$\frac{\partial}{\partial t}\hat{\sigma}_{32} = -\left(\frac{\Gamma+\Gamma_{12}}{2} + i\Delta_c\right)\hat{\sigma}_{32} - \frac{i}{2}(\hat{\sigma}_{22} - \hat{\sigma}_{33})\hat{\Omega}_c^\dagger - \frac{i}{2}\hat{\Omega}_p^\dagger\hat{\sigma}_{12} + \hat{F}_{32}, \tag{3}$$

$$\frac{\partial}{\partial t}\hat{\sigma}_{21} = -\left(\frac{\Gamma_{12}}{2} + \gamma_p + i\delta\right)\hat{\sigma}_{21} + \frac{i}{2}\hat{\Omega}_p^\dagger\hat{\sigma}_{23} - \frac{i}{2}\hat{\sigma}_{31}\hat{\Omega}_c + \hat{F}_{21}, \tag{4}$$

$$\frac{\partial}{\partial t}\hat{\sigma}_{11} = \Gamma_1\hat{\sigma}_{33} + \Gamma_{12}\hat{\sigma}_{22} - \frac{i}{2}\hat{\sigma}_{31}\hat{\Omega}_p + \frac{i}{2}\hat{\Omega}_p^\dagger\hat{\sigma}_{13} + \hat{F}_{11}, \tag{5}$$

$$\frac{\partial}{\partial t}\hat{\sigma}_{22} = \Gamma_2\hat{\sigma}_{33} - \Gamma_{12}\hat{\sigma}_{22} - \frac{i}{2}\hat{\sigma}_{32}\hat{\Omega}_c + \frac{i}{2}\hat{\Omega}_c^\dagger\hat{\sigma}_{23} + \hat{F}_{22}, \tag{6}$$

Optics EXPRESS

$$\frac{\partial}{\partial t}\hat{\sigma}_{33} = -\Gamma\hat{\sigma}_{33} + \frac{i}{2}\hat{\sigma}_{31}\hat{\Omega}_p + \frac{i}{2}\hat{\sigma}_{32}\hat{\Omega}_c - \frac{i}{2}\hat{\Omega}_p^{\dagger}\hat{\sigma}_{13} - \frac{i}{2}\hat{\Omega}_c^{\dagger}\hat{\sigma}_{23} + \hat{F}_{33}, \tag{7}$$

$$\frac{\partial}{\partial t}\hat{\sigma}_{12} = -\left(\frac{\Gamma_{12}}{2} + \gamma_p - i\delta\right)\hat{\sigma}_{12} - \frac{i}{2}\hat{\sigma}_{32}\hat{\Omega}_p + \frac{i}{2}\hat{\Omega}_c^{\dagger}\hat{\sigma}_{13} + \hat{F}_{12}, \tag{8}$$

$$\frac{\partial}{\partial t}\hat{\sigma}_{23} = -\left(\frac{\Gamma + \Gamma_{12}}{2} - i\Delta_c\right)\hat{\sigma}_{23} + \frac{i}{2}(\hat{\sigma}_{22} - \hat{\sigma}_{33})\hat{\Omega}_c + \frac{i}{2}\hat{\sigma}_{21}\hat{\Omega}_p + \hat{F}_{23}, \tag{9}$$

$$\frac{\partial}{\partial t}\hat{\sigma}_{13} = -\left(\frac{\Gamma}{2} - i\Delta_p\right)\hat{\sigma}_{13} + \frac{i}{2}(\hat{\sigma}_{11} - \hat{\sigma}_{33})\hat{\Omega}_p + \frac{i}{2}\hat{\sigma}_{12}\hat{\Omega}_c + \hat{F}_{13}, \tag{10}$$

in which $\hat{F}_{\mu\nu}$ is the corresponding Langevin noise operator, satisfying the fluctuation-dissipation theorem. Γ_{12} is the ground-state population decay rate, and γ_p is the ground-state decoherence rate, both of which can produce entanglement in very similar ways. For simplicity, we set $\gamma_p = 0$ and call Γ_{12} as the ground-state relaxation rate in this work. The field propagations follow the Maxwell-Schrödinger equations given by

$$\left(\frac{1}{c}\frac{\partial}{\partial t} + \frac{\partial}{\partial z}\right)\hat{\Omega}_p = i\left(\frac{\Gamma\alpha}{2L}\right)\hat{\sigma}_{13}, \tag{11}$$

$$\left(\frac{1}{c}\frac{\partial}{\partial t} + \frac{\partial}{\partial z}\right)\hat{\Omega}_c = i\left(\frac{\Gamma\alpha}{2L}\right)\hat{\sigma}_{23}, \tag{12}$$

where L is the medium length, and $\alpha = 4g^2NL/c\Gamma$ is the optical density of atomic medium. N is the total atomic numbers in the ensemble.

Together with atomic equations in Eqs. (2)–(10) and field equations in Eqs. (11) and (12), we have a set of coupled equations between atomic and field operators. To calculate entanglement properties between two fields, we apply the mean-field approximation, dividing each operator $\hat{A}$ into two parts, i.e., $\hat{A} = A + \hat{a}$, where A represents the mean-field value and $\hat{a}$ corresponds to the quantum fluctuation operator. Thus, we can decompose atomic and field operators as $\hat{\sigma}_{\mu\nu} = \sigma_{\mu\nu} + \hat{s}_{\mu\nu}$, $\mu, \nu \in 1, 2, 3$, and $\hat{\mathcal{E}}_\mu = \mathcal{E}_\mu + \hat{a}_\mu$, $\mu \in p, c$, where $\hat{s}_{\mu\nu}$ and $\hat{a}_\mu$ are dimensionless atomic and field fluctuation operators, respectively. The detail derivations are given in Appendix.

In order to quantify the entanglement between two fields, we use Duan's inseparability [47–49], which is a sufficient condition for continuous-variable entanglement demonstrated by many experiments, i.e.,

$$V(\theta) \equiv \Delta^2\left(\hat{X}_p + \hat{X}_c\right)(\theta) + \Delta^2\left(\hat{Y}_p - \hat{Y}_c\right)(\theta) < 4, \tag{13}$$

where $\hat{X}_\sigma = \hat{a}_\sigma e^{-i\theta} + \hat{a}_\sigma^{\dagger} e^{i\theta}$ and $\hat{Y}_\sigma = -i(\hat{a}_\sigma e^{-i\theta} - \hat{a}_\sigma^{\dagger} e^{i\theta})$ are the two quadrature operators of fields $\hat{a}_\sigma$, $\sigma \in p, c$, with the quadrature angle θ. Expressing $V(\theta)$ in terms of field operators, we have

$$V(\theta) = 4\left[1 + \langle\hat{a}_p^{\dagger}\hat{a}_p\rangle + \langle\hat{a}_c^{\dagger}\hat{a}_c\rangle + 2\mathrm{Re}\left(\langle\hat{a}_p\hat{a}_c\rangle e^{-2i\theta}\right)\right]. \tag{14}$$

By scanning all quadrature angles, one can find an optimum quadrature angle θ_{opt}, which minimizes the entanglement quantity V. The entanglement quantity $V(\theta)$ at θ_{opt} is given by

$$V = 4\left[1 + \langle\hat{a}_p^{\dagger}\hat{a}_p\rangle + \langle\hat{a}_c^{\dagger}\hat{a}_c\rangle - 2 \mid \langle\hat{a}_p\hat{a}_c\rangle \mid\right], \tag{15}$$

while $\theta_{\mathrm{opt}} = \left(\mathrm{Arg}\left[\langle\hat{a}_p\hat{a}_c\rangle\right] \pm n\pi\right)/2$, and $n \in$ odd.

The entanglement degree depends on some tunable parameters. In Sec. III, we will show the results of entanglement under various physical quantities, and compare the corresponding entanglement degree.

Optics EXPRESS

3. Numerical results

According to the theoretical model in Sec. II, we know that the entanglement is the function of optical density (α), two-photon detuning (δ), input Rabi-frequency of two fields ($\Omega_{p,c}$), and ground-state relaxation rate (Γ_{12}), which are measurable physical quantities in experiments. For simplicity, we consider asymmetric one-photon detuning, which is arranged as $\Delta_p = -\Delta_c = \delta/2$. In this section, we will compare the two entanglement generation processes: one is by ground-state relaxation rate, and the other one is by two-photon detuning. All the results in this section are obtained numerically.

In Fig. 2(a), we have shown the relation between entanglement quantity V and a ground-state relaxation rate Γ_{12}. For given optical density α and input Rabi frequencies of probe and coupling fields $\Omega_{p,c}$, we can find an optimum ground-state relaxation rate $\Gamma_{12,\mathrm{opt}}$ to maximize the output entanglement (the minimum value of V, i.e., $V_{\mathrm{opt},\Gamma_{12}}$). If we give an optical density and a ground-state relaxation rate, there exists the optimum input Rabi frequency of coupling field $\Omega_{c,\mathrm{opt}}$, such that the output entanglement is maximum ($V_{\mathrm{opt},\Omega_c}$), as shown in Fig. 2(b). EIT condition in Fig. 2 has been used by setting $\Omega_p = 0.1\Omega_c$, and we consider on-resonance case, i.e., two-photon detuning $\delta = 0$.

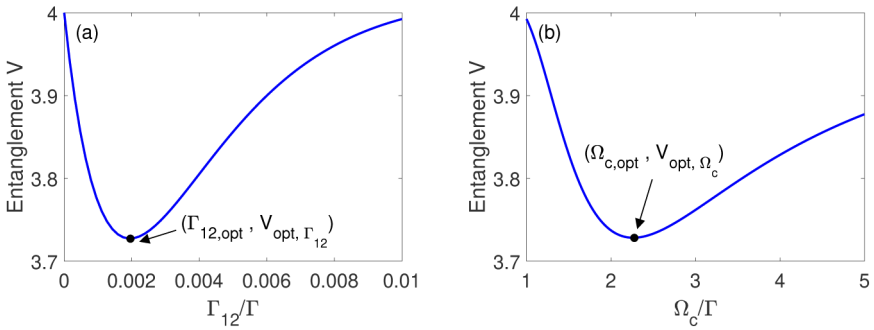

Fig. 2. (a) Entanglement versus ground-state relaxation rate under the parameters given by $\alpha = 1000$ and $\Omega_c = 1\Gamma$. (b) Entanglement versus input coupling Rabi frequency with parameters given by $\alpha = 1000$ and $\Gamma_{12} = 0.01\Gamma$. The input Rabi frequency of probe field is used by setting $\Omega_p = 0.1\Omega_c$, and $\delta = 0$ for the two figures.

Similarly, we consider how the two-photon detuning influences output entanglement. As shown in Fig. 3(a), we can obtain the maximum entanglement by scanning two-photon detuning δ for given optical density and input Rabi frequencies of probe and coupling fields. It is shown that one can find the optimum two-photon detuning δ_{opt} and the corresponding entanglement quantity $V_{\mathrm{opt},\delta}$. With the same process, there exists an optimum $\Omega_{c,\mathrm{opt}}$ to maximize output entanglement, which is $V_{\mathrm{opt},\Omega_c}$ for given α and δ, as shown in Fig. 3(b). As Fig. 2, we have set $\Omega_p = 0.1\Omega_c$ in order to satisfy EIT condition, and we let $\Gamma_{12} = 0$ to ensure that the entanglement is coming from the fact of δ.

From Fig. 2(a) and Fig. 3(a), we can find that no entanglement is generated at output when $\Gamma_{12} = 0 = \delta$, and entanglement between two fields is generated in the presence of Γ_{12} or δ. Compared with the entanglement generated by the two processes, it is clear to see that the entanglement degree is larger and more efficient in two-photon detuning scheme. In addition to the factors of Γ_{12}, δ, and Ω_c, entanglement also depends on the optical density, which is tunable and available in experiments. We are interested in maximum entanglement at different values of α. Figures 4(a) and 4(b) show the results based on the scheme by using Γ_{12}, and the results of δ scheme are depicted in Figs. 4(c) and (d) under various α's. Figure 4(a) illustrates $V_{\mathrm{opt},\Omega_c}$ as a function of Γ_{12}, and the values of $V_{\mathrm{opt},\Omega_c}$ are insensitive to Γ_{12}. For different values of optical

Optics EXPRESS

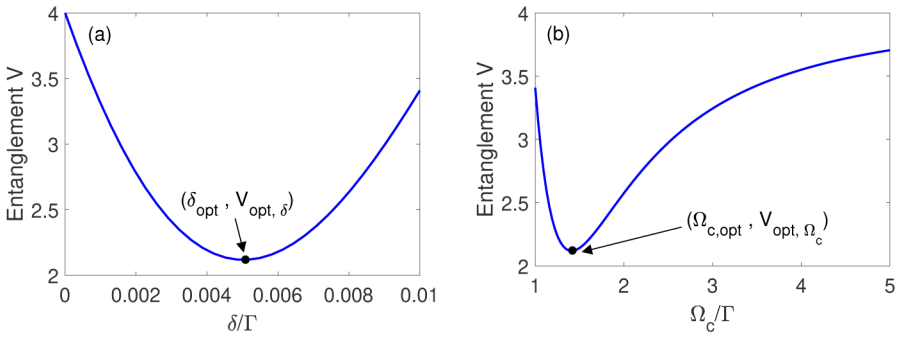

Fig. 3. (a) Entanglement versus two-photon detuning under the parameters given by $\alpha = 1000$ and $\Omega_c = 1\Gamma$. (b) Entanglement versus input coupling Rabi frequency with parameters given by $\alpha = 1000$ and $\delta = 0.01\Gamma$. The input Rabi frequency of probe field is used by setting $\Omega_p = 0.1\Omega_c$, and $\Gamma_{12} = 0$ for the two figures.

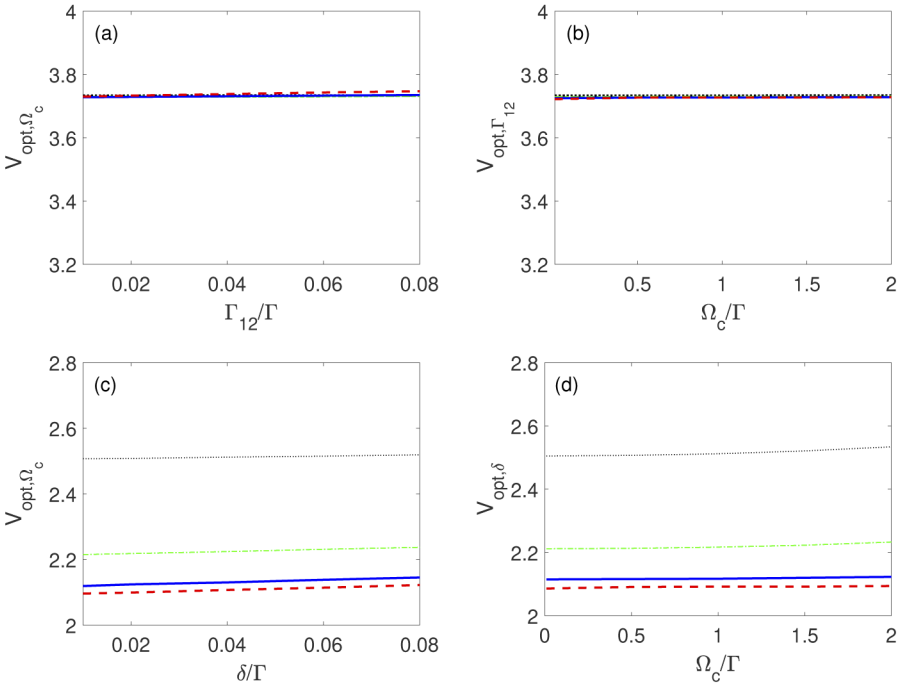

Fig. 4. Optimized entanglement at different α's for the two different processes: by ground state population damping (a) and (b), and by two-photon detuning (c) and (d). Black dotted, green dashed-dotted, blue solid, and red dashed lines represnt α's values of 100, 300, 1000, and 3000, respectively. (a) The minimum value of entanglement quantity obtained by scanning all input Rabi frequencies, V_{opt,Ω_c}, as a function of ground state population damping Γ_{12}. (b) The minimum value of entanglement quantity obtained by scanning all ground state damping, $V_{opt,\Gamma_{12}}$, as a function of input Rabi frequency Ω_c. (c) The minimum entanglement quantity obtained by scanning all input Rabi frequencies, V_{opt,Ω_c}, as a function of two-photon detuning δ. (d) The minimum entanglement quantity obtained by scanning all two-photon detunings, $V_{opt,\delta}$, as a function of input Rabi frequency Ω_c. $\Omega_p = 0.1\Omega_c$ is used in all the figures.

Optics EXPRESS

densities, it shows that the entanglement values do not have significant changes . Similar tendency has been found in $V_{\mathrm{opt},\Gamma_{12}}$, which is insensitive to Ω_c and α, see Fig. 4(b). The entanglement values are around 3.7, just a little smaller than the upper bound value 4. In contrast, Figs. 4(c) and 4(d) illustrate $V_{\mathrm{opt},\Omega_c}$ and $V_{\mathrm{opt},\delta}$ as the functions of δ and Ω_c, respectively. The values of V's are also insensitive to the corresponding variables, but change significantly with α's. The black dotted, green dashed-dotted, blue solid, and red dashed lines represent the values of α's given by 100, 300, 1000, and 3000, respectively. From Figs. 4(c) and (d) , it manifests that the entanglement degree increases when optical density is increasing. The optical density can enhance the output entanglement in the two-photon detuning scheme.

Since the entanglement degree is much larger by using two-photon detuning scheme, we focus on the results of Figs. 4(c) and (d). We can see that the value of optimum entanglement, $V_{\mathrm{opt},\Omega_c}$ and $V_{\mathrm{opt},\delta}$, under a given optical density α is almost a constant.

In Fig. 5, we have numerically plotted the contour plot of entanglement quantity V with respect to Ω_p and δ under three different Ω_c's, which are 0.85Γ, 1.2Γ, and 1.7Γ, respectively. As shown in the three plots, we can see that the values of V are the same, but with different ranges of Ω_p and δ. The positions of Ω_p corresponding to the same values of V is clearly proportional to Ω_c. Similarly, the positions of δ is proportional to Ω_c^2. It implies that there exists a relationship among entanglement quantity V and the ratios of Ω_p/Ω_c and δ/Ω_c^2. The deeper understanding to the results in Fig. 5 will be discussed in Sec. IV.

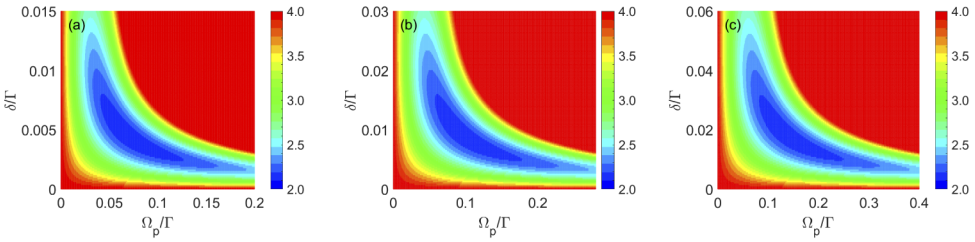

Fig. 5. Contour plot of entanglement quantity V versus Ω_p and δ under different Ω_c's: (a) $\Omega_c = 0.85\Gamma$, (b) $\Omega_c = 1.2\Gamma$, and (c) $\Omega_c = 1.7\Gamma$. For the three plots, optical density is set to be $1,000$. Please note that the ranges of Ω_p and δ are different in the three plots.

4. Discussions

Generation of CV quantum entanglement between probe and coupling fields using atomic EIT system is the key point of this paper. We have proposed a theoretical model in Sec. II, deriving equations of motion for atomic and field operators, and showing the numerical simulation results in Sec.III. In order to understand the physics behind these results thoroughly, in this section we study the system analytically from the framework given in Sec. II. Using Eqs. (2)–(12), one can obtain

$$\frac{\partial}{\partial\zeta}\hat{a}_p = P_1\hat{a}_p + Q_1\hat{a}_p^\dagger + R_1\hat{a}_c + S_1\hat{a}_c^\dagger + \hat{n}_p, \tag{16}$$

$$\frac{\partial}{\partial\zeta}\hat{a}_c = P_2\hat{a}_p + Q_2\hat{a}_p^\dagger + R_2\hat{a}_c + S_2\hat{a}_c^\dagger + \hat{n}_c, \tag{17}$$

where $\zeta \equiv z/L$ is the dimensionless length, and $\hat{n}_p$ and $\hat{n}_c$ are the corresponding Langevin noise operators. P_i, Q_i, R_i, and S_i $(i = 1, 2)$ are the coefficients. For two-photon detuning scheme, i.e.,

Optics EXPRESS

$\Gamma_{12} = 0$, we have

$$\begin{aligned} P_1 &\simeq i\alpha\epsilon - 2\alpha\epsilon^2\ ,\ Q_1 \simeq -2i\alpha\epsilon r^2 e^{2iK\zeta}, \\ R_1 &\simeq -i\alpha\epsilon r e^{iK\zeta}\ ,\ S_1 \simeq -i\alpha\epsilon r e^{iK\zeta}, \\ P_2 &\simeq -i\alpha\epsilon r e^{-iK\zeta}\ ,\ Q_2 \simeq -i\alpha\epsilon r e^{iK\zeta}, \\ R_2 &\simeq i\alpha\epsilon r^2\ ,\ S_2 \simeq 2i\alpha\epsilon r^2, \end{aligned} \tag{18}$$

where $r \equiv |\Omega_p/\Omega_c|$, which is much smaller than 1 under EIT condition i.e., $r \ll 1$. We also have $\epsilon \equiv \Gamma\delta/\Omega_c^2$ and $K \equiv \alpha\epsilon$, where the latter one is the extra phase from probe field. In our analytical study, we assume that the amplitudes of probe and coupling fields are unchanged. It means that r is a constant. Moreover, we don not consider the phase of coupling field because the phase change is very small. Thus, Ω_c is real in our case. On the contrary, we have to take the probe field phase into account. The phase of probe field is $\alpha\epsilon\zeta$, which can be caught from the phase term K in coefficients shown in Eq. (18). The phase term can be eliminated by transforming field operators into a new rotating frame by defining $\hat{O} \rightarrow \hat{O}e^{iK\zeta}$, where $\hat{O}$ represents $\hat{a}_p, \hat{a}_p^\dagger, \hat{n}_p$, and $\hat{n}_p^\dagger$.

Now we turn to consider the entanglement between probe and coupling fields. From Eq. (18), it is clearly to see that the terms of R_1 and S_1 link coupling field operators ($\hat{a}_c$, $\hat{a}_c^\dagger$) and probe field operators ($\hat{a}_p$, $\hat{a}_p^\dagger$); while P_2 and Q_2 make the correlation between probe field operators and coupling field operators. On the other hand, the coefficients of P_1, Q_1, R_2, and S_2 correspond to the self-interaction processes for each field. Let's discuss the physical meaning of these coefficients. First, if there only exists the coefficients of S_1 and Q_2, we can obtain an ideal entangled state, which is coming from two-mode squeezed state formed by $\hat{a}_p$ and $\hat{a}_c$, and the output entanglement is given as $V = 4e^{-2|S|\zeta}$, where $|S_1| = |Q_2| \equiv S$. Second, the physics of the terms of R_1 and P_2 is the cross-phase coupling, which can't produce entanglement at output. Then, when we only consider the coefficients of Q_1 and S_2, which correspond to the single-mode squeezing processes, we can obtain the two independent squeezed lights, for which the entanglement is given by $V = 4\cosh(2|Q_1|\zeta)$. Finally, the coefficients of P_1 and R_2 are related to self-phase or damping/amplification processes, which also do not have the abilities to produce entanglement.

In order to obtain the analytical expression for entanglement, we consider the coefficients coming from the 0^{th} and 1^{st} order terms of r, i.e., P_1, R_1, S_1, P_2, and Q_2, as well as the Langvin noise contributions from $\hat{n}_p$ and $\hat{n}_c$. We yield a form as follows.

$$V_1 = 4\left[1 + \mu^2\left(\frac{e^{-2\lambda} + 2\lambda - 1}{\lambda^2}\right) - 2\mu\left(\frac{1 - e^{-\lambda}}{\lambda}\right)\right], \tag{19}$$

in which $\mu \equiv \alpha\epsilon r$, and $\lambda \equiv 2\alpha\epsilon^2$ is the damping of probe field. When $\lambda \rightarrow 0$, the main contributions are coming from R_1, S_1, P_2, and Q_2, resulting in the entanglement given by $V_1 = 4\left(1 + 2\mu^2 - 2\mu\right)$, which only depends on μ. It implies that $V_{\text{best}} = 2$ when $\mu = 1/2$, which means the entanglement degree is independent of r as long as the condition $\mu = 1/2$. It is quite different from the case of the entanglement by two-mode squeezing, which can approach to an ideal entangled state as $\mu \rightarrow \infty$.

According to Fig. 5, we can plot the entanglement quantity V with respect to r and ϵ. After plotting with the new variables, we can find that the three plots of Figs. 5(a)-(c) correspond to the same result shown in Fig. 6. It implies that V depends only on two independent parameters of ϵ and r, i.e., as long as ϵ and r are given. Any combination of δ, Ω_c, and Ω_p results in the same value of V. One can clearly see that in the plot the condition of $\mu = 1/2$, represented by the dashed line of a hyperbolic function, crosses the minimum or optimum value of V.

However, $\mu = 1/2$ is not a sufficient condition to find the optimum entanglement, and Eq. (19) can't explain our results completely. The main reason for this problem is that the higher order terms of r become important when r is getting large. Thus, we have to consider the terms of

Optics EXPRESS

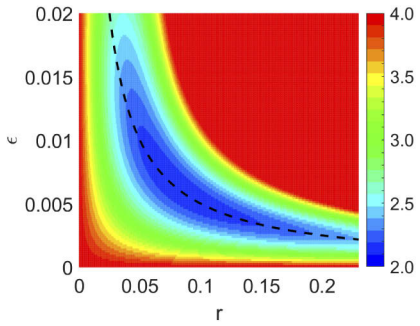

Fig. 6. Contour plot of entanglement quantity V versus r and ϵ. The optical density is given by $\alpha = 1,000$. The black dashed curve is plotted with the condition of $\mu = \alpha\epsilon r = 1/2$.

Q_1 and S_2, which are related to the single-mode squeezing coefficient. According to Eq. (15), one can see that the entanglement degree depends on the average photon numbers of probe and coupling fields. For single-mode squeezed state of probe and coupling, the average photon numbers are $\sinh^2(|Q_1|\zeta)$ and $\sinh^2(|S_2|\zeta)$ rather than 0. As a reason, we can naively modify output entanglement by considering the external photon numbers coming from the single-mode squeezing terms, but without introducing the corresponding extra noises. Thus it reads as

$$V \simeq V_1 + 8\sinh^2(2\mu r). \tag{20}$$

For the case $\lambda \ll 1$, we can expand V_1 to $O(\lambda)$. With these approximations, we can obtain a closed form of output entanglement shown below:

$$V \simeq 4\left(1 + 2\mu^2 - 2\mu\right) + 4\mu\lambda(1 - 4\mu/3) + 8(2\mu r)^2. \tag{21}$$

From Eq. (21), we can obtain the optimum entanglement by substituting $\mu = 1/2$, and express V as the function of α, ϵ, and r by using $\lambda = 2\alpha\epsilon^2$. It will be

$$V_{\text{opt}} = 2 + \frac{4}{3}\alpha\epsilon^2 + 8r^2. \tag{22}$$

According to Eq. (22), we can find the best entanglement by using Lagrangian multiply with the constraint condition given by $\mu = 1/2$. It shows that

$$\epsilon_{\text{opt}} = (3/2)^{1/4}\alpha^{-3/4}, \tag{23}$$

$$r_{\text{best}} = (24\alpha)^{-1/4}. \tag{24}$$

From Eqs. (23) and (24), we can see that ϵ_{opt} and r_{best} are constants when α is given. Under these conditions, the best entanglement value is

$$V_{\text{best}} = 2 + (32/3)^{-1/2}\alpha^{-1/2}, \tag{25}$$

which only depends on optical density α. The result reflects the fact that the value of $\log_{10}(V-2)$ would decrease 0.5 with the increment of an order of magnitude in optical density. It quantitatively matches the results shown in Figs. 4(c) and (d) .

In comparison with the entanglement generation from ground-state dephasing or population decay, we have seen that the scheme of two-photon detuning is more efficient from Fig. 4. The physics behind the result can be understood as follows. For the scheme of ground-state dephasing or population decay, the entanglement coefficients are $|S_1| = |Q_2| = \alpha\varepsilon r e^{-\alpha\varepsilon\zeta}$, where

Optics EXPRESS

$\varepsilon \equiv \Gamma\Gamma_{12}/(2|\Omega_c|^2)$. Since the probe field suffers strong dissipation from Γ_{12}, the entanglement coefficient decays exponentially. However, the depletion rate of probe field due to two-photon detuning is exp $\left(-2\alpha\epsilon^2\zeta\right)$, which is much smaller than that of probe field due to ground-state dephasing or poluation decay, and the entanglement degree $|S_1| = |Q_2| = \alpha\epsilon r e^{-2\alpha\epsilon^2\zeta} \simeq \alpha\epsilon r$. The result implies that the entanglement degree can be enhanced by optical density in two-photon detuning scheme. In contrast, the entanglement degree in ground-state dephasing or population decay scheme is insensitive to optical density, as shown in Figs. 4(a) and (b).

The existence of the optimum ratio r is coming from the competition between dissipation and single-mode squeezing. From Eq. (22), we can rewrite the optimum entanglement as $V_{\rm opt} = 2 + (3\alpha)^{-1}r^{-2} + 8r^2$, from which it is clearly to see that the second and the third terms are attributed to fluctuation noise and single-mode squeezing term, respectively. When r is small, the extra noise dominates the output entanglement value, while the effect of single-mode squeezing term becomes important when r is getting larger. As a result, there exists an optimum value of r to minimize entanglement value V. On the other hand, for given optical density α, the optimum entanglement is given by $V_{\rm opt} = 2 + (4\alpha/3)\epsilon^2 + (2/\alpha^2)\epsilon^{-2}$. It implies that there exists a best entanglement when the sum of extra noise from dissipation and single-mode squeezing is minimized. Generally, two-mode squeezing (S_1, Q_2) and the cross-coupling terms (R_1, P_2) limit the best entanglement to be 2, which is 50% of ideal entangled state. The presence of the probe dissipation P_1 will introduce extra noise fluctuation which is proportional to r^{-2}, and degrade the output entanglement in the region of $r \ll 1$. In contrast, the single-mode squeezing, Q_2 and S_2, will degrade the entanglement degree with extra term being proportional to r^2, which destroys entanglement when r is getting larger. Similarly, we also have optimum ϵ from the condition of $\mu = 1/2$. As a result, we can find the best strength ratio r and detuning-coupling field ratio ϵ to minimize the output entanglement.

5. Conclusion

In the present work, we have discussed the generation of quantum entanglement between probe and coupling fields under EIT condition. We compare the entanglement degree arising from two different mechanisms, which are ground-state relaxation rate and two-photon detuning. Our study has identified that it is more efficient to obtain higher output entanglement degree by introducing two-photon detuning. Furthermore, we have numerically studied the influence of the EIT parameters, which are two-photon detuning, field Rabi frequencies, and optical density to entanglement degree. Also, the conditions of the corresponding parameters for obtaining the optimal entanglement have been found from theoretical analysis. It shows that the two-mode squeezing and cross-coupling terms give us a constraint for the parameters to obtain the best entanglement, i.e. $\mu = 1/2$. The noise fluctuation from probe field dissipation and the single-mode squeezing from probe and coupling fields will reduce the entanglement degree. The optimum condition of r and ϵ for the best entanglement have been found. The study contributes to our understanding of the origin of entanglement induced by atom-field interaction in EIT system, as well as a deeper connection between quantum coherence and entanglement. The work can be further extended to more complicated atomic systems, which have possibilities to produce higher entanglement degree, conducing the progresses in the development of CV quantum information sciences.

Appendix

In this Appendix, we will derive the equations of motion for quantum fluctuations of atomic operators given by Eqs. (2)–(10) as well as the field fluctuations given in Eqs. (11) and (12). By using the mean-field approximation, we can decompose an operator into two parts, which are mean-field part and the corresponding quantum fluctuation part, and one can obtain linear

Optics EXPRESS

equations for fluctuation operators by ignoring the higher-order fluctuation terms. In the following, we have shown the linearized equations of atomic fluctuation operators.

$$\frac{\partial}{\partial t}\hat{s}_{31} = -\left(\frac{\Gamma}{2} + i\Delta_p\right)\hat{s}_{31} - \frac{i}{2}\Omega_p^*(\hat{s}_{11} - \hat{s}_{33}) - \frac{i}{2}g(\sigma_{11} - \sigma_{33})\hat{a}_p^\dagger - \frac{i}{2}\Omega_c^*\hat{s}_{21} - \frac{i}{2}g\sigma_{21}\hat{a}_c^\dagger + \hat{F}_{31}, \tag{26}$$

$$\frac{\partial}{\partial t}\hat{s}_{32} = -\left(\frac{\Gamma + \Gamma_{12}}{2} + i\Delta_c\right)\hat{s}_{32} - \frac{i}{2}\hat{\Omega}_c^*(\hat{s}_{22} - \hat{s}_{33}) - \frac{i}{2}g(\sigma_{22} - \sigma_{33})\hat{a}_c^\dagger - \frac{i}{2}\Omega_p^*\hat{s}_{12} - \frac{i}{2}g\sigma_{12}\hat{a}_p^\dagger + \hat{F}_{32}, \tag{27}$$

$$\frac{\partial}{\partial t}\hat{s}_{21} = -\left(\frac{\Gamma_{12}}{2} + \gamma_p + i\delta\right)\hat{s}_{21} + \frac{i}{2}\Omega_p^*\hat{s}_{23} + \frac{i}{2}g\sigma_{23}\hat{a}_p^\dagger - \frac{i}{2}\sigma_{31}\hat{u}_c - \frac{i}{2}\Omega_c\hat{s}_{31} + \hat{F}_{21}, \tag{28}$$

$$\frac{\partial}{\partial t}\hat{s}_{11} = \Gamma_1\hat{s}_{33} + \Gamma_{12}\hat{s}_{22} - \frac{i}{2}\Omega_p\hat{s}_{31} - \frac{i}{2}g\sigma_{31}\hat{a}_p + \frac{i}{2}\Omega_p^*\hat{s}_{13} + \frac{i}{2}g\sigma_{13}\hat{a}_p^\dagger + \hat{F}_{11}, \tag{29}$$

$$\frac{\partial}{\partial t}\hat{s}_{22} = \Gamma_2\hat{s}_{33} - \Gamma_{12}\hat{s}_{22} - \frac{i}{2}\Omega_c\hat{s}_{32} - \frac{i}{2}g\sigma_{32}\hat{a}_c + \frac{i}{2}\Omega_c^*\hat{s}_{23} + \frac{i}{2}g\sigma_{23}\hat{a}_c^\dagger + \hat{F}_{22}, \tag{30}$$

$$\frac{\partial}{\partial t}\hat{s}_{33} = -\Gamma\hat{s}_{33} + \frac{i}{2}\Omega_p\hat{s}_{31} + \frac{i}{2}g\sigma_{31}\hat{a}_p + \frac{i}{2}\Omega_c\hat{s}_{32} + \frac{i}{2}g\sigma_{32}\hat{a}_c - \frac{i}{2}\Omega_p^*\hat{s}_{13} - \frac{i}{2}g\sigma_{13}\hat{a}_p^\dagger - \frac{i}{2}\Omega_c^*\hat{s}_{23} - \frac{i}{2}g\sigma_{23}\hat{a}_c^\dagger + \hat{F}_{33}, \tag{31}$$

$$\frac{\partial}{\partial t}\hat{s}_{12} = -\left(\frac{\Gamma_{12}}{2} + \gamma_p - i\delta\right)\hat{s}_{12} - \frac{i}{2}\Omega_p\hat{s}_{32} - \frac{i}{2}g\sigma_{32}\hat{a}_p + \frac{i}{2}\sigma_{13}\hat{u}_c^\dagger + \frac{i}{2}\Omega_c^*\hat{s}_{13} + \hat{F}_{12}, \tag{32}$$

$$\frac{\partial}{\partial t}\hat{s}_{23} = -\left(\frac{\Gamma + \Gamma_{12}}{2} - i\Delta_c\right)\hat{s}_{23} + \frac{i}{2}\hat{\Omega}_c(\hat{s}_{22} - \hat{s}_{33}) + \frac{i}{2}g(\sigma_{22} - \sigma_{33})\hat{a}_c + \frac{i}{2}\Omega_p\hat{s}_{21} + \frac{i}{2}g\sigma_{21}\hat{a}_p + \hat{F}_{23}, \tag{33}$$

$$\frac{\partial}{\partial t}\hat{s}_{13} = -\left(\frac{\Gamma}{2} - i\Delta_p\right)\hat{s}_{13} + \frac{i}{2}\Omega_p(\hat{s}_{11} - \hat{s}_{33}) + \frac{i}{2}g(\sigma_{11} - \sigma_{33})\hat{a}_p + \frac{i}{2}\Omega_c\hat{s}_{12} + \frac{i}{2}g\sigma_{12}\hat{a}_c + \hat{F}_{13}, \tag{34}$$

where $\hat{s}_{\mu\nu} = \hat{s}_{\nu\mu}^\dagger$, $\mu, \nu \in 1, 2, 3$. Since we are interested in the steady-state solution for output field operators, we can set the time derivative to be zero. Thus, we can express Eqs. (27)–(34) in the matrix form as $\mathbf{M_1}\,\mathbf{y} + \mathbf{M_2}\,\mathbf{u} + \mathbf{r} = 0$, where $\mathbf{y}^T = (\hat{s}_{31}, \hat{s}_{32}, \hat{s}_{21}, \hat{s}_{11}, \hat{s}_{22}, \hat{s}_{33}, \hat{s}_{12}, \hat{s}_{23}, \hat{s}_{13})$ gives the fluctuations of atomic operators, $\mathbf{a}^T = \left(\hat{a}_p, \hat{a}_p^\dagger, \hat{a}_c, \hat{a}_c^\dagger\right)$ denotes the fluctuations of field operators, and $\mathbf{r}^T = \left(\hat{F}_{31}, \hat{F}_{32}, \hat{F}_{21}, \hat{F}_{11}, \hat{F}_{22}, \hat{F}_{33}, \hat{F}_{12}, \hat{F}_{23}, \hat{F}_{13}\right)$ is the corresponding Langevin

Optics EXPRESS

noise operators, respectively. The matrices $\mathbf{M_1}$ and $\mathbf{M_2}$ are 9 by 9 and 9 by 4 matrix. We have shown the matrix expression as follows.

$$\mathbf{M_1} = \begin{pmatrix} -\tilde{\gamma}_{13}^* & 0 & -i\frac{\Omega_c^*}{2} & -i\frac{\Omega_p^*}{2} & 0 & i\frac{\Omega_p^*}{2} & 0 & 0 & 0 \\ 0 & -\tilde{\gamma}_{23}^* & 0 & 0 & -i\frac{\Omega_c^*}{2} & i\frac{\Omega_c^*}{2} & -i\frac{\Omega_p^*}{2} & 0 & 0 \\ -i\frac{\Omega_c}{2} & 0 & -\tilde{\gamma}_{12}^* & 0 & 0 & 0 & 0 & i\frac{\Omega_p^*}{2} & 0 \\ -i\frac{\Omega_p}{2} & 0 & 0 & 0 & \Gamma_{12} & \Gamma/2 & 0 & 0 & i\frac{\Omega_p^*}{2} \\ 0 & -i\frac{\Omega_c}{2} & 0 & 0 & -\Gamma_{12} & \Gamma/2 & 0 & i\frac{\Omega_c^*}{2} & 0 \\ 0 & 0 & 0 & 1 & 1 & 1 & 0 & 0 & 0 \\ 0 & -i\frac{\Omega_p}{2} & 0 & 0 & 0 & 0 & -\tilde{\gamma}_{12} & 0 & i\frac{\Omega_c^*}{2} \\ 0 & 0 & i\frac{\Omega_p}{2} & 0 & i\frac{\Omega_c}{2} & -i\frac{\Omega_c}{2} & 0 & -\tilde{\gamma}_{23} & 0 \\ 0 & 0 & 0 & i\frac{\Omega_p}{2} & 0 & -i\frac{\Omega_p}{2} & i\frac{\Omega_c}{2} & 0 & -\tilde{\gamma}_{13} \end{pmatrix}_{9\times 9}, \tag{35}$$

$$\mathbf{M_2} = \frac{g}{2}\begin{pmatrix} 0 & -i(\sigma_{11}-\sigma_{33}) & 0 & -i\sigma_{21} \\ 0 & -i\sigma_{12} & 0 & -i(\sigma_{22}-\sigma_{33}) \\ 0 & i\sigma_{23} & -i\sigma_{31} & 0 \\ -i\sigma_{31} & i\sigma_{13} & 0 & 0 \\ 0 & 0 & -i\sigma_{32} & i\sigma_{23} \\ 0 & 0 & 0 & 0 \\ -i\sigma_{32} & 0 & 0 & i\sigma_{13} \\ i\sigma_{21} & 0 & i(\sigma_{22}-\sigma_{33}) & 0 \\ i(\sigma_{11}-\sigma_{33}) & 0 & i\sigma_{12} & 0 \end{pmatrix}_{9\times 4}. \tag{36}$$

in which $\tilde{\gamma}_{13} \equiv \Gamma/2 - i\Delta_p$, $\tilde{\gamma}_{23} \equiv (\Gamma + \Gamma_{12})/2 - i\Delta_c$, and $\tilde{\gamma}_{12} \equiv (\Gamma_{12}/2 + \gamma_p) - i\delta$. The atomic fluctuation operators can be easily expressed in terms of filed operators by solving $\mathbf{y} = -\mathbf{M}_1^{\mathrm{T}}(\mathbf{M}_2\mathbf{a} + \mathbf{r})$.

On the other hand, the field fluctuation equations under steady-state regime are given by

$$\frac{\partial}{\partial\zeta}\hat{a}_p = i\left(\frac{\Gamma\alpha}{2g}\right)\hat{s}_{13}, \tag{37}$$

$$\frac{\partial}{\partial\zeta}\hat{a}_c = i\left(\frac{\Gamma\alpha}{2g}\right)\hat{s}_{23}. \tag{38}$$

where $\zeta \equiv z/L$, which is the normalized distance.

The source terms on right-hand side coming from the atomic coherence operators, which can be directly replaced by field fluctuation operators, i.e. $\hat{s}_{13} = \hat{s}_{13}\left(\hat{a}_p, \hat{a}_p^\dagger, \hat{a}_c, \hat{a}_c^\dagger\right)$, and

Optics EXPRESS

$\hat{s}_{23} = \hat{s}_{23}\left(\hat{a}_p, \hat{a}_p^\dagger, \hat{a}_c, \hat{a}_c^\dagger\right)$. The general expressions of $\hat{s}_{13}$ and $\hat{s}_{23}$ are given as

$$\hat{s}_{13} = A_1\hat{u}_p + B_1\hat{u}_p^\dagger + C_1\hat{u}_c + D_1\hat{u}_c^\dagger + \hat{f}_{13}, \tag{39}$$

$$\hat{s}_{23} = A_2\hat{u}_p + B_2\hat{u}_p^\dagger + C_2\hat{u}_c + D_2\hat{u}_c^\dagger + \hat{f}_{23}. \tag{40}$$

where $\hat{f}_{13}$ and $\hat{f}_{23}$ are the effective Langevin noise operator from Langevin noise operators $\hat{F}_{\mu\nu}$'s given in Eqs. (27)–(34).

The compact form is given as follows.

$$\frac{\partial}{\partial\zeta}\mathbf{a} = \mathbf{C}\mathbf{a} + \mathbf{N} \tag{41}$$

In which $\mathbf{a}^\mathbf{T} \equiv \left(\hat{a}_p, \hat{a}_p^\dagger, \hat{a}_c, \hat{a}_c^\dagger\right)$, and the two matrices of $\mathbf{C}$ and $\mathbf{N}$ have the explicit form as

$$\mathbf{C} = i\frac{\Gamma\alpha}{2}\begin{pmatrix} A_1 & B_1 & C_1 & D_1 \\ -B_1^* & -A_1^* & -D_1^* & -C_1^* \\ A_2 & B_2 & C_2 & D_2 \\ -B_2^* & -A_2^* & -D_2^* & -C_2^* \end{pmatrix} \equiv \begin{pmatrix} P_1 & Q_1 & R_1 & S_1 \\ Q_1^* & P_1^* & S_1^* & R_1^* \\ P_2 & Q_2 & R_2 & S_2 \\ Q_2^* & P_2^* & S_2^* & R_2^* \end{pmatrix}, \tag{42}$$

$$\mathbf{N} = i\frac{\Gamma\alpha}{2g}\begin{pmatrix} \hat{f}_{13}, -\hat{f}_{13}^\dagger, \hat{f}_{23}, -\hat{f}_{23}^\dagger \end{pmatrix}^T. \tag{43}$$

The correlations between two field fluctuation operators can be calculated from Eq. (41). It is straightforwardly to have the form as follows.

$$\frac{\partial}{\partial\xi}\mathbf{S} = \mathbf{C}\mathbf{S} + \mathbf{S}\mathbf{C}^\dagger + \mathbf{Z}. \tag{44}$$

Here, $\mathbf{S} \equiv \langle\mathbf{a}\mathbf{a}^\dagger\rangle$, and the matrix $\mathbf{Z}$ shows the correlations of Langevin noise operators, denoted $\langle\mathbf{N}\mathbf{N}^\dagger\rangle$. That is

$$\mathbf{Z} \equiv \langle\mathbf{N}\mathbf{N}^\dagger\rangle = \frac{\Gamma\alpha}{4}\left(\mathbf{V}\mathcal{D}\mathbf{V}^\dagger\right). \tag{45}$$

Here, we have to consider the correlations of any two Langevin noise operators, i.e., $\langle\hat{F}_\mu\hat{F}_\nu\rangle = \mathcal{D}_{\mu\nu}\, c/(NL)$, in which $\mathcal{D}_{\mu\nu}$ is the diffusion coefficient obtained from general Einstein relation. By solving Eq. (44), one can calculate the entanglement degree based on Eq. (15) with the matrix elements of $\mathbf{S}$:

$$V = 4\left(1 + \mathbf{S}_{22} + \mathbf{S}_{44} - 2\left|\mathbf{S}_{14}\right|\right). \tag{46}$$

Funding. Ministry of Science and Technology (105-2628-M-007-003-MY4, 106-2119-M-007-003, 107-2745-M-007-001, 109-2112-M-007- 019-MY3, 108-2639-M-007-001-ASP, 109-2639-M-007-002-ASP).

Disclosures. The authors declare no conflicts of interest.

References

1. A. Furusawa, J. L. Sørensen, S. L. Braunstein, C. A. Fuchs, H. J. Kimble, and E. S. Polzik, "Unconditional Quantum Teleportation," Science **282**(5389), 706–709 (1998).
2. L. S. Madsen, V. C. Usenko, M. Lassen, R. Filip, and U. L. Andersen, "Continuous variable quantum key distribution with modulated entangled states," Nat. Commun. **3**(1), 1083 (2012).
3. D. Bouweester, A. Ekert, and A. Zeilinger, *The Physics of Quantum Information* (Springer-Verlag, 2000).
4. S. L. Braunstein and P. van Loock, "Quantum information with continuous variables," Rev. Mod. Phys. **77**(2), 513–577 (2005).
5. M. A. Nielsen and I. L. Chuang, *Quantum Computation and Quantum Information* (Cambridge University, 2000).

Optics EXPRESS

6. N. Korolkova, G. Leuchs, R. Loudon, T. C. Ralph, and C. Silberhorn, "Polarization squeezing and continuous-variable polarization entanglement," Phys. Rev. A **65**(5), 052306 (2002).
7. W. P. Bowen, N. Treps, R. Schnabel, and P. K. Lam, "Experimental Demonstration of Continuous Variable Polarization Entanglement," Phys. Rev. Lett. **89**(25), 253601 (2002).
8. V. Josse, A. Dantan, A. Bramati, M. Pinard, and E. Giacobino, "Continuous Variable Entanglement using Cold Atoms," Phys. Rev. Lett. **92**(12), 123601 (2004).
9. V. Josse, A. Dantan, A. Bramati, and E. Giacobino, "Entanglement and squeezing in a two-mode system: theory and experiment," J. Opt. B: Quantum Semiclassical Opt. **6**(6), S532–S543 (2004).
10. M. Lassen, G. Leuchs, and U. L. Andersen, "Continuous Variable Entanglement and Squeezing of Orbital Angular Momentum States," Phys. Rev. Lett. **102**(16), 163602 (2009).
11. K. Wagner, J. Janousek, V. Delaubert, H. Zou, C. Harb, N. Treps, J. F. Morizur, P. K. Lam, and H. A. Bachor, "Entangling the Spatial Properties of Laser Beams," Science **321**(5888), 541–543 (2008).
12. V. Boyer, A. M. Marino, R. C. Pooser, and P. D. Lett, "Entangled Images from Four-Wave Mixing," Science **321**(5888), 544–547 (2008).
13. V. Boyer, A. M. Marino, and P. D. Lett, "Generation of Spatially Broadband Twin Beams for Quantum Imaging," Phys. Rev. Lett. **100**(14), 143601 (2008).
14. M. D. Reid and P. D. Drummond, "Quantum Correlations of Phase in Nondegenerate Parametric Oscillation," Phys. Rev. Lett. **60**(26), 2731–2733 (1988).
15. Z. Y. Ou, S. F. Pereira, H. J. Kimble, and K. C. Peng, "Realization of the Einstein-Podolsky-Rosen paradox for continuous variables," Phys. Rev. Lett. **68**(25), 3663–3666 (1992).
16. F. Jinxia, W. Zhenju, L. Yuanji, and Z. Kuanshou, "Generation of 8.3 dB continuous variable quantum entanglement at a telecommunication wavelength of 1550 nm," Laser Phys. Lett. **15**(1), 015209 (2018).
17. W. P. Bowen, R. Schnabel, P. K. Lam, and T. C. Ralph, "Experimental Investigation of Criteria for Continuous Variable Entanglement," Phys. Rev. Lett. **90**(4), 043601 (2003).
18. G. Masada, K. Miyata, A. Politi, T. Hashimoto, J. L. O'Brien, and A. Furusawa, "Continuous-variable entanglement on a chip," Nat. Photonics **9**(5), 316–319 (2015).
19. C. F. McCormick, V. Boyer, E. Arimondo, and P. D. Lett, "Strong relative intensity squeezing by four-wave mixing in rubidium vapor," Opt. Lett. **32**(2), 178–180 (2007).
20. C. F. McCormick, A. M. Marino, V. Boyer, and P. D. Lett, "Strong low-frequency quantum correlations from a four-wave-mixing amplifier," Phys. Rev. A **78**(4), 043816 (2008).
21. R. C. Pooser, A. M. Marino, V. Boyer, K. M. Jones, and P. D. Lett, "Low-Noise Amplification of a Continuous-Variable Quantum State," Phys. Rev. Lett. **103**(1), 010501 (2009).
22. Q. Glorieux, R. Dubessy, S. Guibal, L. Guidoni, J.-P. Likforman, T. Coudreau, and E. Arimondo, "Double-Λ microscopic model for entangled light generation by four-wave mixing," Phys. Rev. A **82**(3), 033819 (2010).
23. Q. Glorieux, L. Guidoni, S. Guibal, J.-P. Likforman, and T. Coudreau, "Quantum correlations by four-wave mixing in an atomic vapor in a nonamplifying regime: Quantum beam splitter for photons," Phys. Rev. A **84**(5), 053826 (2011).
24. J. D. Swaim and R. T. Glasser, "Squeezed-twin-beam generation in strongly absorbing media," Phys. Rev. A **96**(3), 033818 (2017).
25. R. Ma, W. Liu, Z. Qin, X. Jia, and J. Gao, "Generating quantum correlated twin beams by four-wave mixing in hot cesium vapor," Phys. Rev. A **96**(4), 043843 (2017).
26. Z. Qin, L. Cao, H. Wang, A. M. Marino, W. Zhang, and J. Jing, "Experimental Generation of Multiple Quantum Correlated Beams from Hot Rubidium Vapor," Phys. Rev. Lett. **113**(2), 023602 (2014).
27. J. Xin, J. Qi, and J. Jing, "Enhancement of entanglement using cascaded four-wave mixing processes," Opt. Lett. **42**(2), 366–369 (2017).
28. F. Hudelist, J. Kong, C. Liu, J. Jing, Z. Y. Ou, and W. Zhang, "Quantum metrology with parametric amplifier-based photon correlation interferometers," Nat. Commun. **5**(1), 3049 (2014).
29. M. Fleischhauer, A. Imamoğlu, and J. P. Marangos, "Electromagnetically induced transparency: Optics in coherent media," Rev. Mod. Phys. **77**(2), 633–673 (2005).
30. L. V. Hau, S. E. Harris, Z. Dutton, and C. H. Behroozi, "Light speed reduction to 17 metres per second in an ultracold atomic gas," Nature **397**(6720), 594–598 (1999).
31. C. Liu, Z. Dutton, C. H. Behroozi, and L. V. Hau, "Observation of coherent optical information storage in an atomic medium using halted light pulses," Nature **409**(6819), 490–493 (2001).
32. M. Fleischhauer and M. D. Lukin, "Quantum memory for photons: Dark-state polaritons," Phys. Rev. A **65**(2), 022314 (2002).
33. Y. F. Chen, C. Y. Wang, S. H. Wang, and I. A. Yu, "Low-Light-Level Cross-Phase-Modulation Based on Stored Light Pulses," Phys. Rev. Lett. **96**(4), 043603 (2006).
34. Y.-L. Chuang, I. A. Yu, and R.-K. Lee, "Quantum theory for pulse propagation in electromagnetically-induced-transparency media beyond the adiabatic approximation," Phys. Rev. A **91**(6), 063818 (2015).
35. Y.-L. Chuang, R.-K. Lee, and I. A. Yu, "Optical-density-enhanced squeezed-light generation without optical cavities," Phys. Rev. A **96**(5), 053818 (2017).
36. Z.-Y. Liu, Y.-H. Chen, Y.-C. Chen, H.-Y. Lo, P.-J. Tsai, I. A. Yu, Y.-C. Chen, and Y.-F. Chen, "Large Cross-Phase Modulations at the Few-Photon Level," Phys. Rev. Lett. **117**(20), 203601 (2016).

Optics EXPRESS

37. C. L. Garrido Alzar, L. S. Cruz, J. G. Aguirre Gómez, M. Franç, A. Santos, and P. Nussenzveig, "Super-Poissonian intensity fluctuations and correlations between pump and probe fields in Electromagnetically Induced Transparency," Europhys. Lett. **61**(4), 485–491 (2003).
38. P. Barberis-Blostein and N. Zagury, "Field correlations in electromagnetically induced transparency," Phys. Rev. A **70**(5), 053827 (2004).
39. P. Barberis-Blostein, "Field autocorrelations in electromagnetically induced transparency: Effects of a squeezed probe field," Phys. Rev. A **74**(1), 013803 (2006).
40. F. Wang, X. Hu, W. Shi, and Y. Zhu, "Entanglement between collective fields via phase-dependent electromagnetically induced transparency," Phys. Rev. A **81**(3), 033836 (2010).
41. M. Paternostro, M. S. Kim, and B. S. Ham, "Generation of entangled coherent states via cross-phase-modulation in a double electromagnetically induced transparency regime," Phys. Rev. A **67**(2), 023811 (2003).
42. M. D. Lukin and A. Imamoğlu, "Nonlinear Optics and Quantum Entanglement of Ultraslow Single Photon," Phys. Rev. Lett. **84**(7), 1419–1422 (2000).
43. X. Yang, J. Sheng, U. Khadka, and M. Xiao, "Generation of correlated and anticorrelated multiple fields via atomic spin coherence," Phys. Rev. A **85**(1), 013824 (2012).
44. X. Yang, Y. Zhou, and M. Xiao, "Generation of multipartite continuous-variable entanglement via atomic spin wave," Phys. Rev. A **85**(5), 052307 (2012).
45. X. Yang, Y. Zhou, and M. Xiao, "Entangler via electromagnetically induced transparency with an atomic ensemble," Sci. Rep. **3**(1), 3479 (2013).
46. X. Yang and M. Xiao, "Electromagnetically Induced Entanglement," Sci. Rep. **5**(1), 13609 (2015).
47. L.-M. Duan, G. Giedke, J. I. Cirac, and P. Zoller, "Inseparability Criterion for Continuous Variable Systems," Phys. Rev. Lett. **84**(12), 2722–2725 (2000).
48. R. Simon, "Peres-Horodecki Separability Criterion for Continuous Variable Systems," Phys. Rev. Lett. **84**(12), 2726–2729 (2000).
49. Y. L. Chuang and R.-K. Lee, "Conditions to preserve quantum entanglement of quadrature fluctuation fields in electromagnetically induced transparency media," Opt. Lett. **34**(10), 1537–1539 (2009).